Coherent splitting of Bose-Einstein condensed atoms with optically-induced Bragg diffraction

M. Kozuma†, L. Deng‡, E.W. Hagley, J. Wen, R. Lutwak*, K. Helmerson,

S. L. Rolston, and W. D. Phillips

National Institute of Standards and Technology - Gaithersburg, Maryland 20899

ABSTRACT We have observed Bragg diffraction of a Bose-Einstein condensate of sodium atoms by a moving, periodic, optical potential. The coherent process of Bragg diffraction produced a splitting of the condensate with unidirectional momentum transfer. Using the momentum selectivity of the Bragg process, we separated a condensate component with a momentum width narrower than that of the original condensate. By repeatedly pulsing the optical potential while the atoms were trapped, we observed the trajectory of the split atomic wave packets in the confining magnetic potential.

Atom optics, the manipulation of atoms in analogy to the control of light with optical elements, has seen rapid advances in recent years. Of particular interest are applications that rely on the deBroglie wave nature of the atoms, such as diffraction and interferometry [1]. An important technique of atom optics is Bragg diffraction by an optical standing wave [2-4]. It provides coherent splitting of matter waves with unidirectional momentum transfer. With the advent of Bose-Einstein Condensation (BEC) of dilute atomic gases [5-8], a coherent source of matter waves analogous to an optical laser is now available for atom optics. Bragg diffraction preserves the condensate's coherence properties while providing efficient, selectable momentum transfer. In this Letter, we report Bragg diffraction of a Bose-Einstein condensate of sodium atoms by a moving, periodic optical potential**.**

We believe Bragg diffraction will be a versatile technique for manipulating Bose-Einstein condensates. For example, it will be useful as an output coupler for an atom laser [9] because the large momentum transfer produces a directed output beam and the process is coherent [10]. The technique for producing Bragg diffracted wave packets can be used to manipulate a condensate in a trap, creating multiple, coherent components whose interaction and interference can be studied. The Bragg process is also sensitive to the initial momentum of an atomic wave packet, allowing one to impart a well defined momentum to the condensate while having a negligible effect on the uncondensed fraction. This may allow studies of the interactions between the condensed and non-condensed portions of the gas, such as damping, or atom-atom scattering stimulated by bosonic enhancement.

When an atomic beam passes through a periodic optical potential formed by a standing light wave, and interacts with it for a sufficiently long time, it can Bragg diffract in a manner similar to the Bragg diffraction of x-rays from a thick crystal. In each case the incident beam must satisfy a condition on the angle of incidence. Our Bragg diffraction is instead performed on a stationary Bose condensate. In contrast to the Bragg diffraction of an atomic beam, the interaction time is determined not by the passage of the

atoms through a standing wave, but by the duration of a laser pulse. The condition on the angle of incidence becomes a condition on the frequency difference between the two beams comprising the standing wave, or equivalently, the velocity of the moving standing wave. Bragg diffraction under these conditions can also be thought of as stimulated optical Compton scattering [11], a recoil-induced resonance [12,13], or more conveniently as a stimulated Raman transition between two momentum states.

n-th order Bragg diffraction by a moving, optical standing wave can be viewed as a 2n-photon stimulated Raman process in which photons are absorbed from one beam and stimulated to emit into the other (Fig 1b). The Raman picture allows us to think of the initial and final momentum states as an effective two-level system coupled by the multi-photon Raman process. Conservation of energy and momentum require

$$\frac{(nP_{\text{recoil}})^2}{2M} = n\hbar\delta_n, \qquad (1)$$

where $P_{\text{recoil}} = 2\hbar k \sin(\theta/2)$ is the recoil momentum that the atom receives from a two-photon Raman process, $k = 2\pi/\lambda$, λ is the wavelength of the light, M is the atomic mass, and δ_n is the frequency difference between the two lasers. For our conditions first-order Bragg diffraction is resonant at $\delta_1/2\pi$ = 98 kHz and higher orders at $\delta_n = n\delta_1$.

In our experiment, we first produce a BEC as described in detail elsewhere [14]. Briefly, about 10^{10} sodium atoms are optically cooled and trapped in a dark MOT [15]. The atoms are then transferred into a magnetic quadrupole field where atoms in the $3S_{1/2}$ F=1, m_F=-1 state are trapped, compressed, and then cooled by rf-induced evaporation. Before the atoms are lost in the zero field region in the center of the quadrupole field, a TOP [16] magnetic trap is created by suddenly turning on a rotating bias field. The TOP bias field rotates in the x-z plane, where x is the quadrupole axis, and z is vertical along the direction of gravity. Our TOP trap differs from the original design of [16] in that our bias field rotates in a plane that includes the quadrupole symmetry axis. For a constant-magnitude rotating bias field the ratio between

spring constants along the x, y, and z directions is $K_x:K_y:K_z = 4:2:1$. The atoms are further compressed in the TOP trap and cooled by evaporation to well below the transition temperature. We obtain a condensate with about 10^6 sodium atoms having no discernible uncondensed fraction in a trap with harmonic frequencies of $\omega_x / 2\pi = 360\,\text{Hz}$, $\omega_y / 2\pi = 250\,\text{Hz}$, $\omega_z / 2\pi = 180\,\text{Hz}$.

Our first experiments were performed on Bose-condensed atoms released suddenly from the TOP trap. The magnetic trap is turned off in 50 μs and the condensate undergoes a burst of expansion driven by the mean-field repulsion between the atoms. After a few characteristic times, $\tau = \left(\omega_x \omega_y \omega_z\right)^{-1/3}$, the mean field becomes negligible and the cloud expands ballistically [17]. During this ballistic expansion period the condensate is exposed to a moving, periodic optical potential. This potential is generated by two nearly counter-propagating ($\theta = 166^\circ$) laser beams with parallel linear polarizations but slightly different frequencies (Fig. 1a). These (phase coherent) laser beams are derived from a single laser (λ = 589 nm) using acousto-optic modulators. The intensity of each beam is 23 mW/cm^2, and the common detuning with respect to the $3S_{1/2}$, F=1 → $3P_{3/2}$, F'=2 transition is Δ/2π = -1.85 GHz. To transfer the maximum number of atoms to the desired momentum state, we empirically choose laser intensities and pulse durations to give a π-pulse for the effective two-level system. We use two nearly counter-propagating pulses with laser frequencies ω and ω+δ that overlap for 55 μs [18]. The probability of an atom spontaneously emitting a photon during the pulses is less than 0.05.

Figure 2a is an absorption image taken just before the Bragg pulse is applied. The atoms are first optically pumped into the $3S_{1/2}$ F=2 ground-state. They are then absorption-imaged [5] with probe light that drives the $F=2 \rightarrow F'=3$ transition. The probe propagates opposite to gravity and is orthogonal to the plane that contains the Bragg beams. From different time-of-flight images taken after the mean field becomes negligible, we determine the rms momentum width of the released condensate. Along the direction of the Bragg momentum transfer we measure $\Delta P_{\text{rms}} = 0.30\,(4)\,\hbar k$ (all uncertainties here and

elsewhere in this paper represent one standard deviation combined statistical and systematic uncertainties). Fig. 2b, 2c and 2d are images taken at 2.2 ms, 5.6 ms and 10 ms, respectively, after the beginning of the Bragg pulse (which occurs 2 ms after the condensate is released). Here, we can clearly see that a slice is removed from the center of the atomic momentum distribution and is displaced by $P_{\mathrm{recoil}} \sim 2\hbar k$. The slice appears because the resonant width of the Raman transition in momentum space is narrower than ΔP_{rms} of the condensate. From these images, we have determined the rms momentum of Bragg diffracted atoms along the direction of the momentum transfer to be 0.16 (1) $\hbar k$. The expected resonant width of the Bragg diffraction can be calculated from an integration of the optical Bloch equations for a two-level system with a time dependent two-photon Rabi frequency. In our case, the calculated peak two-photon Rabi frequency is $\Omega_2/2\pi$ = 30 kHz, and the predicted momentum width is 0.08 $\hbar k$, a factor of 2 less than what was measured. We do not have an explanation for the excess measured width, although it may be due in part to residual mean field effects [19].

This analysis implies that we can Bragg diffract the entire cloud of atoms if the pulse duration τ is short enough such that $\tau^{-1} >> 2k\Delta P_{\mathrm{rms}} / M$, and the intensity is sufficient for a π-pulse. To achieve this we reduce the rms momentum width of the condensate by adiabatically expanding the trap. The axial gradient of the quadrupole field is linearly ramped down from 9.2 T/m to 0.71 T/m in 2 s while the TOP bias field is increased from 1.0 mT to 1.2 mT. This reduces the frequencies, ω_i, of the TOP trap by factor of 14. Even for this weak trap, the size of the condensate is determined almost entirely by the mean-field interaction. In this Thomas-Fermi limit, the asymptotic momentum spread of the released condensate decreases as $\omega^{3/5}$ [20]. The rms momentum width of the released condensate after adiabatic cooling should therefore be one-fifth the momentum width of a condensate released from the tight trap. This is in qualitative agreement with the observed expansion in time-of-flight images. (The adiabatically expanded condensate is so cold that it undergoes very little expansion during the time of flight, therefore its

momentum spread cannot be accurately measured.)

After adiabatic expansion, the condensate is abruptly released from the TOP trap and allowed to expand for 2 ms. The Bragg pulse of counter-propagating laser beams is then applied and the atoms are imaged 5.6 ms later. When the difference δ between the two laser frequencies is zero, Eq. (1) is not satisfied and diffraction does not occur (Fig. 3a) because the Fourier transform width of the 55 μs pulse is small compared to 98 kHz. When $\delta / 2\pi$ = 98 kHz, first-order Bragg diffraction (Fig. 3b), with up to 100% efficiency, is observed. In Fig. 3b we intentionally chose the diffraction efficiency to be less than 100% so that the original position of the condensate remained visible. Figures 3c and 3d show second and third-order Bragg diffraction, where $\delta / 2\pi$ is 200 kHz, 300 kHz and the intensities are 230 mW/cm^2, 340 mW/cm^2, respectively. The efficiency of third order Bragg diffraction was observed to be as high as 45%. When the sign of the frequency difference δ is reversed, atoms are diffracted into the opposite direction as seen in Fig. 3e. With longer pulses we have observed up to sixth order Bragg diffraction with a momentum transfer of 11.9 $\hbar k$ (corresponding to a velocity of 0.35 m/s) and an efficiency of about 15%. For such a high-order process we cannot achieve a high transfer efficiency with our choice of detuning because the required pulse length and intensities make the probability of spontaneous emission near unity. Figure 3f provides a graphic demonstration of spontaneous emission. The ring pattern results from dipole emission of atoms illuminated by a single traveling wave. Here the direction of observation is along the laser polarization. The center of the ring is displaced by $\hbar k$ due to absorption.

In Bragg diffraction the internal state remains unchanged, so the temporal variations of the Zeeman shift due to the rotating bias field of the TOP trap are unimportant. This is true provided the Zeeman shifts are small compared to the detuning of the laser from the optical transition, as in our case. We can therefore use Bragg diffraction in the trap to study the motion of trapped atoms. Figure 4 shows an example of this where we created a train of orbiting wave packets. In the adiabatically expanded TOP trap we irradiate the

condensate with a series of 13 Bragg pulses, each separated in time by 5 ms. The 13 wave packets and the remaining condensate are then imaged with a single probe pulse. In order to generate many atomic wave packets without substantially depleting the condensate, we decrease the pulse duration of the moving standing wave to 20 μs, reducing the efficiency of Bragg diffraction. Here the crossing angle of the laser beams is 90° and the frequency difference is $\delta / 2\pi$ = 50 kHz to satisfy the first-order Bragg condition. Since the trap potential is non-central, atoms launched along a direction (45° with respect to x and y in this case) other than a principal axis will not execute closed orbits, as seen in Fig. 4. The orbit of the wave packets agrees well with the classical equations of motion for a particle moving in our harmonic trap potential with its incommensurate frequencies [21].

In summary, we have demonstrated coherent Bragg diffraction of Bose-Einstein condensed sodium atoms. This technique, demonstrated both with and without the trapping fields, can be used to manipulate condensates and to study fundamental aspects of their properties. For example it is possible to measure the coherence time of a condensate. While the magnetic trap is held on, atoms may be launched along a principal axis. The diffracted wave packet will return to the condensate after an integral number of half-oscillation periods. The application of a second Bragg pulse when the diffracted wave packet and the original condensate overlap would produce interference, allowing a measurement of the coherence time in the trap. If, on the other hand, the magnetic trap is switched off, the phase of the condensate will start to evolve because the mean-field repulsion is no longer balanced by the magnetic trap potential. Consequently, successive application of Bragg pulses could be used to probe the temporal evolution of the condensate phase (here one would apply the second Bragg pulse before the first wavepacket leaves the region of the condensate). Experiments on non-linear atom optics are also possible using these techniques. For example four-wave mixing of matter waves should occur due to the non-linearity arising from atom-atom interactions [22,23]. Repeated Bragg diffraction allows one to create the three different momentum states of a

condensate necessary to produce a fourth momentum component. A multi-photon Raman process like Bragg diffraction is also ideal for the development of an output coupler for an atom laser. Output coupling with momentum transfer should produce an extremely well collimated beam of coherent atoms.

The authors thank C.W. Clark, M. Doery, M.A. Edwards, P.S. Julienne, J. Lawall and Y. Ovchinnikov for their valuable comments and suggestions. M.K. acknowledges the support of the Japanese Society for the Promotion of Science for Young Scientists. This work was supported in part by the Office of Naval Research and NASA.

References

† Current address: Department of Physics, Tokyo University, Japan.

‡ Permanent address: Department of Physics, Georgia Southern University, GA

* Current address: FTS, Inc., MA

[1]. See, for example, the special issue on atom interferometry, Applied Physics B **54**, 321(1992).

[2] P.J. Martin, B.G. Oldaker, A.H. Miklich, and D.E. Pritchard, Phys. Rev. Lett. **60**, 515 (1988).

[3] D.M. Giltner, R.W. McGowan, and S.A. Lee, Phys. Rev. A **52**, 3966 (1995); M.K. Oberthaler, R. Abfalterer, S. Bernet, J. Schmiedmayer, and A. Zeilinger, Phys. Rev. Lett. **77**, 4980 (1996).

[4] S. Kunze, S. Dürr, and G. Rempe, Europhys. Lett. **34**, 343 (1996).

[5] M.H. Anderson, J.R. Ensher, M.R. Matthews, C.E. Wieman and E.A. Cornell, Science **269**, 198 (1995).

[6] K.B. Davis, M.-O. Mewes, M.R. Andrews, N.J. van Druten, D.S. Durfee, D.M. Kurn, and W. Ketterle, Phys. Rev. Lett. **75**, 3969 (1995).

[7] C.A. Sackett, H.T.C. Stoof, and R.G. Hulet, Phys. Rev. Lett. **80**, 2031 (1998). (See also, C.C. Bradley, C.A. Sackett, J.J. Tollett, and R.G. Hulet, Phys. Rev.) Lett. **75**, 1687 (1995).

[8] D.G. Fried, T.C. Killian, L.Willmann, D. Landhuis, S.C. Moss, D. Kleppner and T.J. Greytak, Phys. Rev. Lett. **81**, 3807, (1998).

[9] M.-O. Mewes, M.R. Andrews, D.M. Kurn, D.S. Durfee, C.G. Townsend and W. Ketterle, Phys. Rev. Lett., **78**, 582, (1997)

[10] D.M. Giltmer, R.W. McGowan, and S.A. Lee, Phys. Rev. Lett. **75**, 2638 (1995).

[11] D.R. Meacher, D. Boiron, H. Metcalf, C. Salomon, and G. Grynberg, Phys. Rev. A **50**, R1992 (1994).

[12] J-Y. Courtois, G. Grynberg, B. Lounis, and P. Verkerk, Phys. Rev. Lett. **72**, 3017(1994).

[13] M. Kozuma, K. Nakagawa, W. Jhe, and M. Ohtsu, Phys. Rev. Lett. **76**, 2428 (1996).

[14] R. Lutwak, L. Deng, M. Gatzke, E.W. Hagley, M. Kozuma, J. Müller, A. Steinberg, R. Thompson, J. Wen, K. Helmerson, S.L. Rolston, and W.D. Phillips, (to be published).

[15] W. Ketterle, K.B. Davis, M.A. Joffe, A. Martin, and D.E. Pritchard, Phys. Rev. Lett. **70**, 2253 (1993).

[16] W. Petrich, M.H. Anderson, J.R. Ensher, and E.A. Cornell, Phys. Rev. Lett. **74**, 3352 (1995).

[17] C.W. Clark, private communication, (1998).

[18] The counter-propagating pulses are triangular with rise and fall times of 40 μs. There is a 25 μs delay between them. Although this pulse sequence was chosen for adiabatic passage experiments there is no adiabatic transfer in our case. The Raman process happens only during the 55 μs overlap.

[19] M. Doery, private communication, (1998).

[20] F. Dalfovo, S. Giorgini, L.P. Pitaevskii, S. Stringari, (to be published in Rev. Mod. Phys.)

[21] M. Edwards, private communication (1998).

[22] E.V. Goldstein, K. Plättner, P. Meystre, J. Res. Natl. Inst. Stand. Technol. **101**, 4, 583 (1996).

[23] M. Trippenbach, Y.B. Band, and P.S. Julienne, (to be published).

Figure Captions

Figure 1 Experimental arrangement of the laser beams (a) and partial transition diagram (b) for *n*-th order Bragg diffraction. The parabolas correspond to the $P^2/2M$ kinetic energy.

Figure 2 Optical absorption images of Bragg diffracted condensates. (a) an image taken just before the moving standing wave pulse is applied. (b), (c), and (d) are taken 2.2 ms, 5.6 ms, and 10 ms after the pulse, respectively. (e) is a profile taken over a horizontal line in the center of the expanding clouds. (d). The width of the field of view is 1.4 mm $\times$ 0.5 mm.

Figure 3 Optical depth images of condensates which were first adiabatically expanded and then Bragg diffracted. (a), (b), (c), (d) and (e) are images taken 5.6 ms after Bragg pulses with frequency differences of $\delta / 2\pi$ = 0 kHz, 98 kHz, 200 kHz, 300 kHz, and -98 kHz respectively. (f) is an image where spontaneous emission occurred using a single laser beam. The width of the field of view is 2.3 mm $\times$ 0.5 mm.

Figure 4 Optical depth image of the condensate after 13 Bragg pulses while in the TOP trap. Here **x** is quadrupole axis and **z** is the direction of gravity. The TOP bias field rotates in the **x**-**z** plane. The Bragg diffraction beams propagate along the **x** and -**y** directions. The width of the field of view is 1.2 mm $\times$ 1.2 mm.

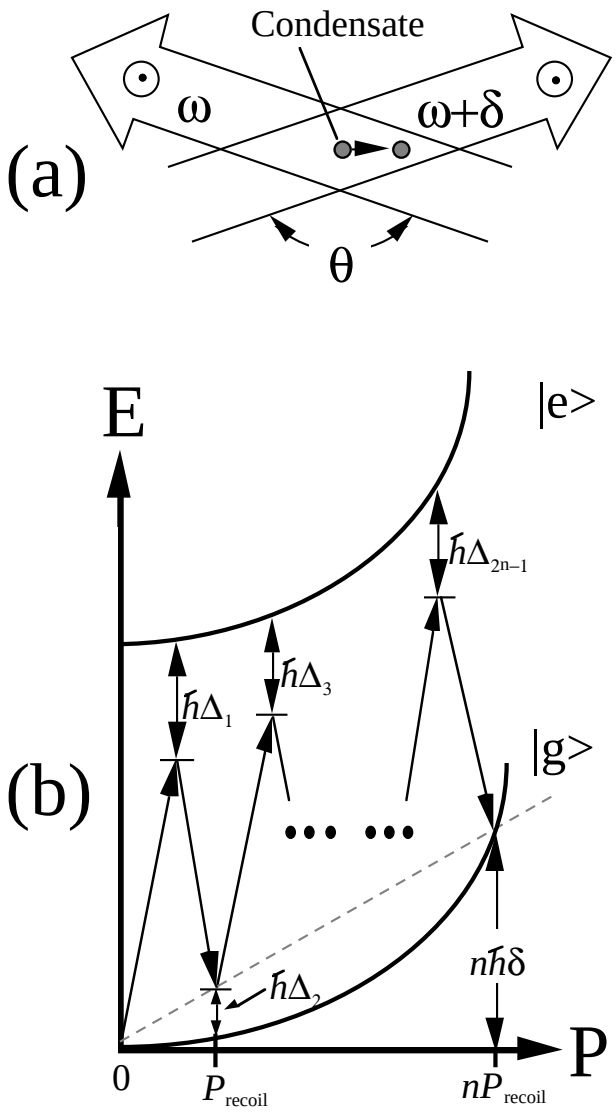
Condensate
ω
ω+δ
(a)
θ
E
|e>
ħΔ2n–1
ħΔ3
ħΔ1
(b)
|g>
nħδ
ħΔ2
P
0
Precoil
nPrecoil

Figure 1

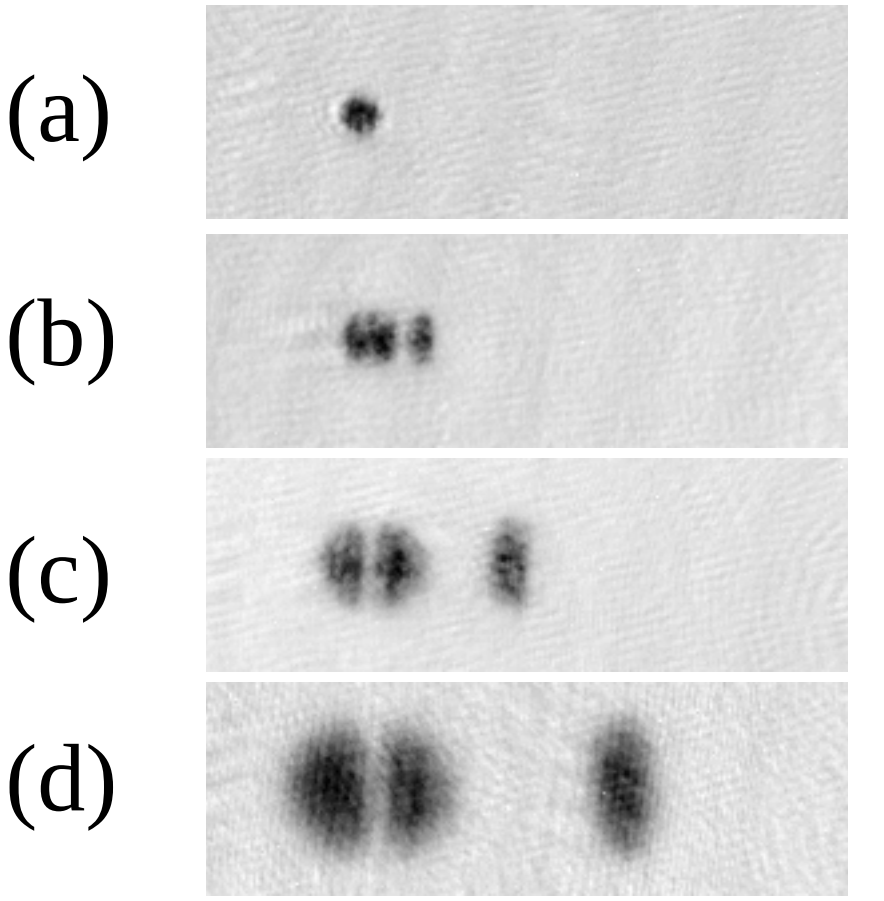
(a)
(b)
(c)
(d)
(e)
$\Delta P_{rms} = 0.16\ (1)\ \hbar k$
1.45
Optical Depth
0
0
1.4
Spatial axis
(mm)

Figure 2

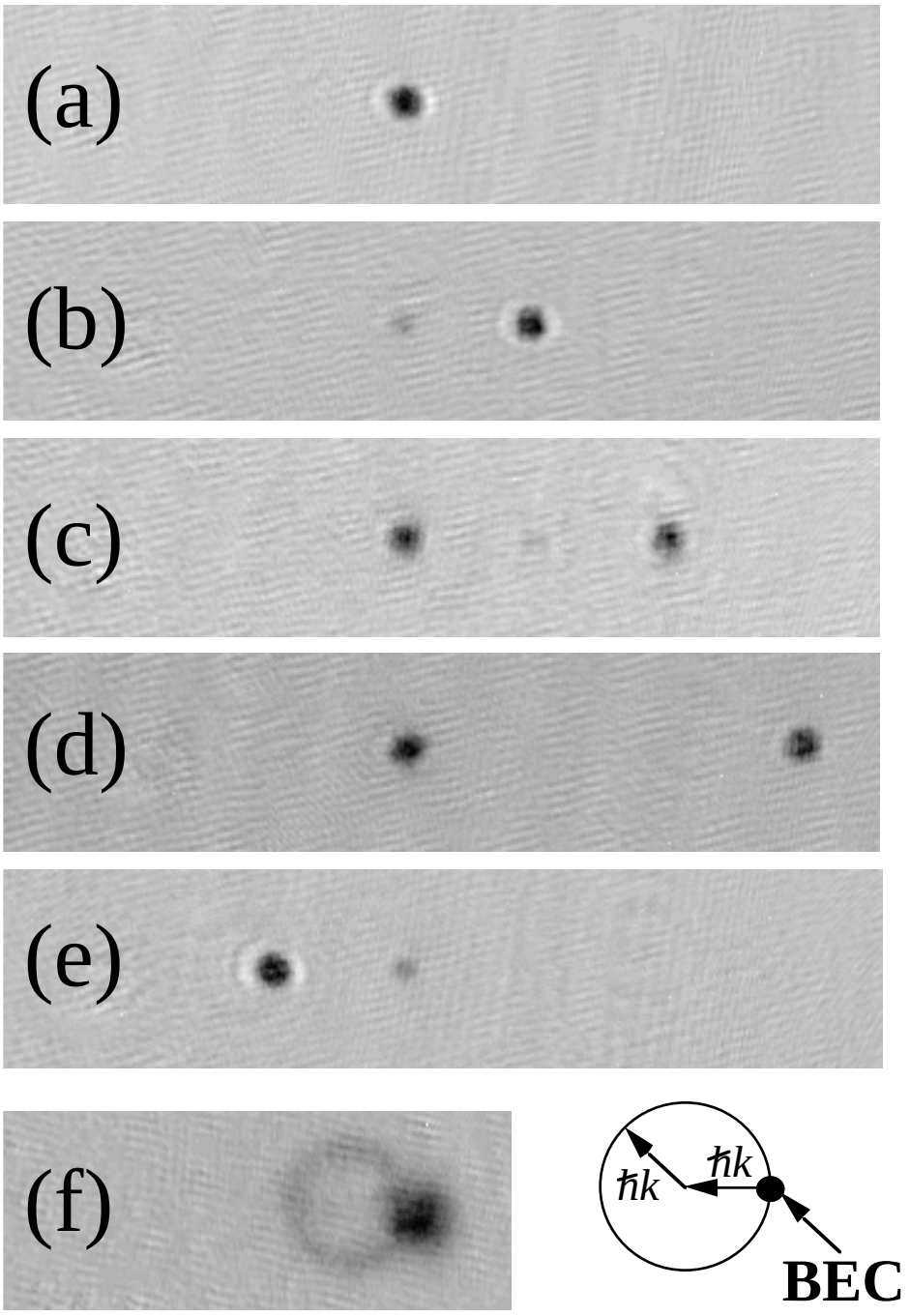

Figure 3

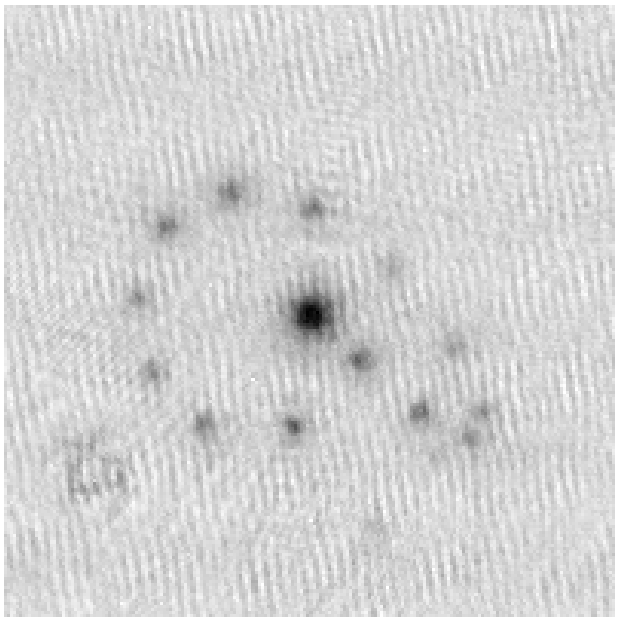

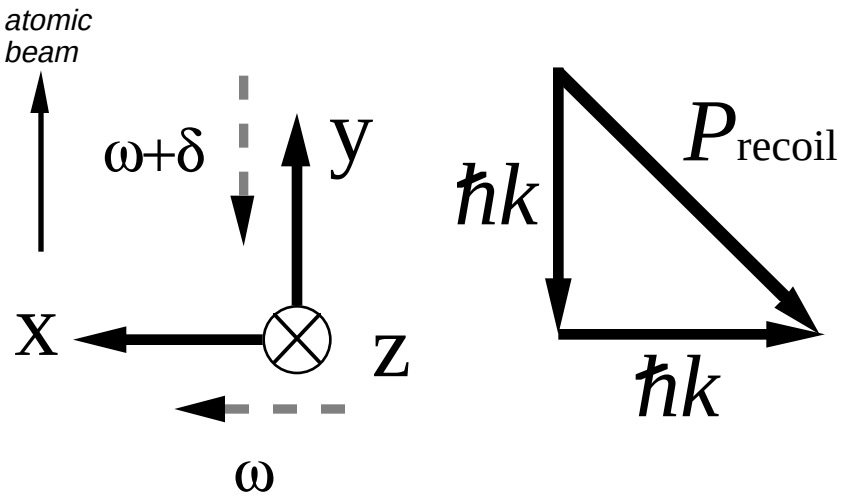

Figure 4